 Bull. Chem. Soc. Jpn. Vol. 83, No. 4, 351–363 (2010)

The Evaluation Theory of Free Radical Scavenging and the Application to Xanthine Oxidase#

Keiichi Mitsuta

Intellectual Property Group, Common Engineering Center, JEOL Ltd.,
1-2 Musashino 3-chome, Akishima, Tokyo 196-8558

Received November 25, 2009; E-mail: mitsuta@jeol.co.jp

A competitive reaction theory in which flexibility is given to the orders of reaction has been established. As a result of an analysis based on this novel theory, the stoichiometric coefficients of the reactions between superoxide dismutase (SOD) and superoxide radicals ($O_2^{-\bullet}$), between xanthine oxidase (XOD) and $O_2^{-\bullet}$, and between 5,5-dimethyl-1-pyrroline *N*-oxide (DMPO) and $O_2^{-\bullet}$ have all been estimated to be 1:1. Furthermore, the hitherto unknown second-order rate constant for the reaction between XOD and $O_2^{-\bullet}$ has been estimated to be 1.4×10^6 or ca. $8.0 \times 10^5\,M^{-1}\,s^{-1}$. It is considered that the presence of the SOD-*like* activity possessed by XOD itself is one of the causes of the puzzling fact reported that the amount of $O_2^{-\bullet}$ observed in a xanthine–XOD system is smaller than the anticipated amount by one order of magnitude. In addition, this SOD-*like* activity of XOD may cause researchers to underestimate the rate constant for the reaction between $O_2^{-\bullet}$ and a spin-trapping agent when the spontaneous dismutation of $O_2^{-\bullet}$ in the presence of XOD was used as a competitor against the spin-trapping reaction for $O_2^{-\bullet}$.

The competitive reaction method is a method for precisely determining an unknown reaction rate constant as a value relative to the reaction rate constant of a reference substance by taking a reacted substance having a known reaction rate constant as the reference substance and by causing a reacted substance having an unknown reaction rate constant to react competitively with a given reacting substance.[1]

In recent years, the kinetic investigation between short-lived free radicals and free radical scavengers has been performed by employing such a competitive reaction method and by applying ESR spin-trapping.[2] The ESR spin-trapping technique is used to detect unstable short-lived free radical species after converting into semi-stable spin adducts by reacting with a spin-trapping agent, and to observe the adducts by using ESR spectroscopy.

In general, spin-trapping agents have a double-bonded site within each molecule. Radicals are selectively trapped at those sites. A reaction between radicals ($R^\bullet$) and the spin-trapping agent (T:) is typically represented as follows:

$$R^\bullet + :T \xrightarrow{k_T} \underset{\text{(spin adducts)}}{R-T^\bullet} \xrightarrow{k_D} \text{decomposition products} \quad (1)$$

where k_T is the trapping rate constant of radicals, k_D is the decomposition rate constant of spin adducts, $\bullet$ are unpaired electrons of radicals R, and : are π-electron pairs at radical-trapping sites in the spin-trapping agents T.

The first research in which competitive reactions were applied to spin-trapping was conducted in 1979 by Finkelstein and co-workers.[3] In this research, SOD (superoxide dismutase) was used as the reference substance. The rate constant for the reaction between superoxide radicals [$O_2^{-\bullet}/HO_2^\bullet$ (hereinafter abbreviated $O_2^{-\bullet}$)] and the spin-trapping agent DMPO (5,5-dimethyl-l-pyrroline *N*-oxide) was precisely determined.

In 1980, the research conducted by Finkelstein and co-workers evolved into a project to determine the rate constants for the reaction between DMPO and $O_2^{-\bullet}$ at various values of pH.[4] According to the same papers, they also succeeded in determining the rate constants for the reactions between hydroxyl radicals ($HO^\bullet$) and various spin-trapping agents by competitive reaction using ethanol as a reference substance.

In 1983, Makino and co-workers observed competitive reactions among various spin-trapping agents and scavengers for hydrogen radicals ($H^\bullet$) and $HO^\bullet$ produced from water by means of ultrasonic irradiation, and showed that the concentration response to inhibition of generation of spin adducts arising from the competitive reactions shows an S-shaped curve relative to the scavenger concentration.[5]

In 1986, a research group at Okayama University and JEOL Ltd. discovered that an S-shaped curve similar to the S-shaped curve discovered by Makino and co-workers appeared in a competitive reaction between DMPO and SOD for $O_2^{-\bullet}$.[6] They also showed that the SOD-*like* activity in a biological sample can be quantified by a competitive reaction with DMPO while using the S-shaped curve as a calibration line.[7,8] This research then evolved into a study in 1992 about aging, that indicated that the SOD-*like* activities of human cerebrospinal fluid and rat brain tissue are enhanced with advancing age.[9]

In 1988, Miyagawa and co-workers succeeded in quantifying the SOD activity within rat serum using DMPO, based on a Stern–Volmer type linear calibration line instead of an S-shaped curve.[10] In this research, methods of linearly plotting SOD activity which were developed by Sawada and Yamazaki in 1973[11] and by Nishikimi in 1975,[12] which were then used in optical absorption spectroscopy, were converted to a spin-trapping method.

Published on the web March 26, 2010; doi:10.1246/bcsj.20090311

From 1988 to 1990, a research group from JEOL Ltd. and Okayama University first succeeded in theoretically explaining the S-shaped inhibitory curve on generation of spin adducts observed during a competitive reaction between DMPO and SOD for $O_2^{-\bullet}$. Furthermore, they succeeded in observing the saturation level of trapped $O_2^{-\bullet}$. Thus, the saturation phenomena of the amount of trapped $O_2^{-\bullet}$ observed by optical absorption spectroscopy by Sawada and Yamazaki in 1973[11] and by Nishikimi in 1975[12] were also confirmed by spin-trapping. In addition, a successful attempt was made to compare scavengers in terms of the SOD-*like* activity value by competitively reacting SOD and superoxide scavengers other than SOD with DMPO systematically and representing their SOD-*like* activities using indices (or, reaction rate constants) based on the ID_{50} (inhibitory dose fifty) of the generation of spin adducts.[13–16]

Triggered by these initial successes, research employing ESR spin-trapping on superoxide scavengers,[17–24] on hydroxyl radical scavengers,[24–27] on nitric monoxide radical (NO) scavengers,[28–30] on alkoxyl radical (R–O$^\bullet$) scavengers,[31,32] and on alkylperoxyl radical (R–OO$^\bullet$) scavengers[31] were reported one after the other. With respect to the S-shaped curve, more sophisticated theories were then proposed by Mitsuta and coworkers.[22,33] A technique for evaluating the reactivity of scavengers by spin-trapping making use of a competitive reaction has been introduced in a recently published forum review on spin-trapping methods.[34] Today, this technique has come to occupy an important position as an area of application of ESR.

Regarding how data are interpreted in the first paper of the present author[15] and how the theory in the second paper[22] is advanced, some items should be added, and others, evolved. It is to be hoped that spin-trapping employing competitive reactions will be further developed theoretically by successive discussion of the additions and evolutions. In the present paper, discussion is started by establishing the appendix theory in the second paper and concluded by solving one unsolved problem in the first paper. Furthermore, the established theories are applied to measure the superoxide scavenging activity of xanthine oxidase (XOD) by using ESR spin-trapping.

Although XOD is known to be a superoxide generating enzyme, there is one unsolved problem about the reactivity between $O_2^{-\bullet}$ and XOD. One of the aims of this work is to solve such unsolved problems of XOD on the basis of both experiments and theories.

Experimental

Materials. The spin-trapping agent 5,5-dimethyl-1-pyrroline *N*-oxide (DMPO, a colorless liquid, Mitsui Toatsu Chemicals), cuprozinc superoxide dismutase (Cu,Zn-SOD, bovine erythrocyte, a pale blue solid, 3300 unit/mg protein, Boehringer Mannheim), xanthine oxidase (XOD, cow's milk, a light brown suspension, 20 unit/mL, Boehringer Mannheim), potassium superoxide (KO_2, a yellow powder containing superoxide anion, Aldrich Chemical), 1,4,7,10,13,16-hexaoxacyclooctadecane (18-crown-6 ether, a colorless crystalline solid of a phase transfer catalyst, Aldrich Chemical), and the stable nitroxide radical 4-hydroxy-2,2,6,6-tetramethylpiperidine-1-oxyl (TEMPOL, an orange crystalline solid, Sigma Chemical) were used. The other chemicals used were of the highest grade commercially available. These substances were used without further purification.

Instruments. ESR spectra were recorded on a JEOL JES-RE1X spectrometer using a quartz flat cell. The interior dimensions of the cell were 60 mm × 10 mm × 0.31 mm and its effective volume was 160 μL. This ESR spectrometer was equipped with an X-band-type cylindrical TE_{011} mode cavity resonator. Optical absorption spectra were measured using a Hitachi U-2000 spectrophotometer.

Measurement of Spin Adduct Generation Inhibitory Response Curves Using SOD and a Hypoxanthine–XOD System. DMPO spin-trapping data was derived by our previously reported method.[15,22] A total volume of 150 μL of a system for the superoxide generation was prepared and dissolved in 100 mM (1 M = 1 mol dm^{-3}) phosphate buffer solution (pH 7.8). The system consisted of 50 μL of 2.0 mM hypoxanthine, 35 μL of 5.5 mM diethylenetriamine-*N*,*N*,*N*′,*N*′′,*N*′′-pentaacetic acid (DTPA), 15 μL of DMPO, and 50 μL of various concentrations of Cu,Zn-SOD prepared by serial double dilution. Then, 50 μL of freshly prepared 0.33 unit/mL XOD was added to the system and reacted. This reaction mixture contained 0.50 mM hypoxanthine, 0.96 mM DTPA, 0.67 M DMPO, 0.083 unit/mL XOD, and a given concentration of Cu,Zu-SOD as the final concentrations. The mixtures were then transferred to a quartz flat cell. Finally, the signal intensity of spin adducts occurring after a lapse of 85 s from the start of the reaction was observed using an ESR spectrometer. A sensitivity correction of the ESR spectrum was made to the obtained data using a manganese marker (Mn^{2+} in MgO).[35] The enzyme activity of Cu,Zn-SOD has been previously confirmed by the method of McCord and Fridovich.[36]

Measurement of Spin Adduct Generation Inhibitory Response Curves Using XOD and a KO_2 System. DMPO spin-trapping data was derived by our previously reported method.[22] Various concentrations of XOD prepared by serial double dilution were first dissolved in 200 μL of 100 mM phosphate buffer solution (pH 7.8). Then, 15 μL of DMPO, followed by 10 μL of freshly prepared ca. 6 mM KO_2 in dimethyl sulfoxide (DMSO) solution including 12 mM 18-crown-6 ether were added to the system and reacted. This reaction mixture contained 0.60 M DMPO, 4.4% volume of DMSO, 0.53 mM 18-crown-6 ether, and a given concentration of XOD as the final concentrations. The mixtures were then transferred to a quartz flat cell. Finally, the signal intensity of spin adducts occurring after a lapse of 30 s from the start of the reaction was observed using an ESR spectrometer. A sensitivity correction of the ESR spectrum was made to the obtained data using a manganese marker (Mn^{2+} in MgO).[35] The molar concentration of the XOD has been previously determined by optical absorption spectroscopy, based on a molar absorption coefficient ($\varepsilon = 37800\,M^{-1}\,cm^{-1}$) of enzyme-bounded FAD at 450 nm.[37]

Measurement of Saturation Level Curves on Generation of Spin Adducts Using DMPO. DMPO spin-trapping data was derived by our previously reported method.[15] A total volume of 150 μL of a system for the superoxide generation was prepared and dissolved in 100 mM phosphate buffer solution (pH 7.8). The system consisted of 50 μL of 2.0 mM hypoxanthine, 35 μL of 5.5 mM DTPA, and 65 μL of various concentrations of DMPO preferably prepared by serial double dilution. Then, 50 μL of freshly prepared 0.33 unit/mL XOD was added to the system and reacted. This reaction mixture contained 0.50 mM hypoxanthine, 0.96 mM DTPA, 0.083 unit/mL XOD, and a given concentration of DMPO as the final concentrations. The mixtures were then transferred to a quartz flat cell. Finally, the signal intensity of spin adducts occurring after a lapse of 85 s from the start of the reaction

was measured using an ESR spectrometer. A sensitivity correction of the ESR spectrum was made to the obtained data using a manganese marker (Mn^{2+} in MgO).[35] The absolute concentration of observed spin adduct was determined by a double integration of the ESR spectrum. To obtain quantitative spin concentrations, 1 μM TEMPOL aqueous solution was used for a primary standard of the double-integrated ESR absorption.[15,22]

Results and Discussion

Establishment of a General Theory Roughly Sketched out in the Appendix of a Paper Published in 1994 by the Present Author and Co-workers. The appendix theory[22] is a general theory in which aggregation behavior was introduced in both of two independent competitive reactions. Competitive reactions of a spin-trapping agent (T) and a scavenger (S) with radicals ($R^\bullet$) are generally represented by the following two non-stoichiometric reactions:

$$m_1R^\bullet + n_1T \xrightarrow{k_T^*} (T_{n_1}R_{m_1}) \quad (2)$$

and

$$m_2R^\bullet + n_2S \xrightarrow{k_S^*} (S_{n_2}R_{m_2}) \quad (3)$$

As is well known, a reaction rate equation cannot be deduced from a net reaction like eq 2 or 3. Here, the author naively assumes their rate equations as:

$$\frac{d[(T_{n_1}R_{m_1})]}{dt} = k_T^*[T]^{n_1}[R^\bullet]^{m_1} \quad (4)$$

and

$$\frac{d[(S_{n_2}R_{m_2})]}{dt} = k_S^*[S]^{n_2}[R^\bullet]^{m_2} \quad (5)$$

Where no scavenger is contained in the system, radicals are consumed by a reaction of eq 2. However, if a scavenger is added to the system, some of the radicals consumed by the reaction of eq 2 are consumed by the radical scavenging reaction of eq 3. Let X ($0 < X < 1$) be the ratio of radicals consumed by the radical scavenging reaction to the total amount of radicals consumed. When a scavenger is added, the ratio of radicals trapped and consumed by the spin-trapping agent within the system can be represented as decreasing to $(1 - X)$. Furthermore, the rate of consumption of the radicals depends on the ratios $(1 - X)$ and X at which the radicals are quenched by the molecules of the spin-trapping agent T and the scavenger S, respectively, and on the orders of reaction m_1 and m_2 of the radicals themselves. Therefore, the ratio of rates of consumption of the radicals $R^\bullet$ induced by the reaction rate eqs 4 and 5 can be represented as $(1 - X)^{m_1}:X^{m_2}$. It can be said from reaction eqs 2 and 3 that consumption of 1 mol of radicals $R^\bullet$ produces reaction products consisting of $1/m_1$ mole of $(T_{n_1}R_{m_1})$ and $1/m_2$ mole of $(S_{n_2}R_{m_2})$. Finally, the ratio of the reaction rates (4) and (5) to the rates of consumption of radicals $R^\bullet$ are represented as follows according to a simple mass law.

$$-\frac{d[R^\bullet]}{dt}:\frac{d[(T_{n_1}R_{m_1})]}{dt}:\frac{d[(S_{n_2}R_{m_2})]}{dt} = 1:\frac{1}{m_1}(1-X)^{m_1}:\frac{1}{m_2}X^{m_2} \quad (6)$$

Equations 4, 5, and 6 lead to

$$k_T^*[T]^{n_1}[R^\bullet]^{m_1}:k_S^*[S]^{n_2}[R^\bullet]^{m_2} = \frac{1}{m_1}(1-X)^{m_1}:\frac{1}{m_2}X^{m_2} \quad (7)$$

In order to facilitate evolving equations used later, a constant A is introduced such that $k_T^*[T]^{n_1}[R^\bullet]^{m_1} = (A/m_1)(1 - X)^{m_1}$ holds. Then, eq 7 is rewritten into the form:

$$k_T^*[T]^{n_1}[R^\bullet]^{m_1}:k_S^*[S]^{n_2}[R^\bullet]^{m_2} = \frac{A}{m_1}(1-X)^{m_1}:\frac{A}{m_2}X^{m_2} \quad (8)$$

When the relationship $a:b = c:d$ holds, if $a = c$, then $b = d$. Therefore, if the left-side terms a and c are raised to the power of m_2 and the right-side terms b and d are raised to the power of m_1, the equality $a^{m_2}:b^{m_1} = c^{m_2}:d^{m_1}$ also holds. Accordingly, eq 8 results in

$$\{k_T^*[T]^{n_1}[R^\bullet]^{m_1}\}^{m_2}:\{k_S^*[S]^{n_2}[R^\bullet]^{m_2}\}^{m_1} = \left\{\frac{A}{m_1}(1-X)^{m_1}\right\}^{m_2}:\left\{\frac{A}{m_2}X^{m_2}\right\}^{m_1} \quad (9)$$

Because the product of the internal terms is equal to the product of the external terms, eq 9 can be modified into

$$k_S^{*m_1}[S]^{n_2m_1}[R^\bullet]^{m_1m_2}\cdot\frac{A^{m_2}}{{m_1}^{m_2}}(1-X)^{m_1m_2} = k_T^{*m_2}[T]^{n_1m_2}[R^\bullet]^{m_1m_2}\cdot\frac{A^{m_1}}{{m_2}^{m_1}}X^{m_1m_2} \quad (10)$$

Rearranging eq 10 gives rise to

$$k_S^{*m_1} = k_T^{*m_2}\cdot A^{m_1-m_2}\cdot\frac{{m_1}^{m_2}}{{m_2}^{m_1}}\cdot\frac{X^{m_1m_2}}{(1-X)^{m_1m_2}}\cdot\frac{[T]^{n_1m_2}}{[S]^{n_2m_1}} \quad (11)$$

In our experiments on competitive reactions, the concentration of the spin-trapping agent was kept constant, while the scavenger concentration was varied. Therefore, when $X = 0.5$, i.e., when 50% of the radicals within the system are consumed by the spin-trapping agent and the remaining 50% by the scavenger, eq 11 can be simplified into the following form by introducing ID_{50} (inhibitory dose fifty) into the variable scavenger concentration:

$$k_S^{*m_1} = k_T^{*m_2}\cdot A^{m_1-m_2}\cdot\frac{{m_1}^{m_2}}{{m_2}^{m_1}}\cdot\frac{[T]^{n_1m_2}}{{ID_{50}}^{n_2m_1}} \quad (12)$$

If the introduction of an approximate relationship $m_1 = m_2 = n_1 = n_2 = 1$ is permitted, eq 12 can be simplified into the form:

$$k_S = k_T\cdot\frac{[T]}{ID_{50}} \quad (13)$$

From eq 13, k_S can be easily calculated roughly as the second-order rate constant for the reaction, based on [T], k_T, and ID_{50} of the scavenger. This approximated second-order rate constant, k_S, will become a good measure of reactivity when the reactivity between each radical species and each scavenger molecule is examined. This is a significant point of this theory looked at from the viewpoint of practical use.

By comparing and combining eqs 11 and 12, the following eq 14 or eq 15 is derived:

$$[S]^{n_2} = \frac{X^{m_2}}{(1-X)^{m_2}}\cdot{ID_{50}}^{n_2} \quad (14)$$

or

Table 1. Theoretically Calculated Values Illustrating the S-Shape of Competitive Reaction Curves (When $I_0 = ID_{50} = 1$)

Rate of scavenging X	I: Rate of trapping $(1-X)$	[S]: $\frac{X}{(1-X)}$	$\left\{\frac{X}{(1-X)}\right\}^2$	$\left\{\frac{X}{(1-X)}\right\}^{1/2}$
0.01	0.99	0.0101	0.0001	0.1005
0.05	0.95	0.0526	0.0028	0.2294
0.10	0.90	0.1111	0.0123	0.3333
0.15	0.85	0.1765	0.0312	0.4201
0.20	0.80	0.2500	0.0625	0.5000
0.25	0.75	0.3333	0.1111	0.5774
0.30	0.70	0.4286	0.1837	0.6547
0.35	0.65	0.5385	0.2900	0.7338
0.40	0.60	0.6667	0.4444	0.8165
0.45	0.55	0.8182	0.6695	0.9045
0.50	0.50	1.0000	1.0000	1.0000
0.55	0.45	1.2222	1.4938	1.1055
0.60	0.40	1.5000	2.2500	1.2247
0.65	0.35	1.8571	3.4488	1.3628
0.70	0.30	2.3333	5.4443	1.5275
0.75	0.25	3.0000	9.0000	1.7321
0.80	0.20	4.0000	16.000	2.0000
0.85	0.15	5.6667	32.110	2.3805
0.90	0.10	9.0000	81.000	3.0000
0.95	0.05	19.000	361.00	4.3589
0.99	0.01	99.000	9801.0	9.9499

$$[S] = \frac{X^f}{(1-X)^f} \cdot ID_{50} \tag{15}$$

where the new factor f ($f = m_2/n_2$) is defined as the apparent number of radicals that one molecule of scavenger can scavenge. That is, aggregation behavior appears only on the scavenger side in this situation. In the experiments, the concentration of the spin-trapping agent was kept constant, and so m_1 and n_1, which are parameters indicating the aggregation behavior of the spin-trapping agent are not reflected in the form of the S-curve.

Spin adduct concentrations $[(T_{n_1}R_{m_1})]$ obtained in the presence and absence of the scavenger S are replaced by the signal intensities of the observed spin adducts $(T_{n_1}R_{m_1})$ represented by I and I_0, respectively. On the basis of how I and I_0 are defined, their relationship is given by

$$I = (1-X) \cdot I_0 \tag{16}$$

The X in eqs 14 and 15 is used as a parameter for connecting I and [S]. Under the three conditions $f = 1$, 2, and 1/2, normalization $I_0 = ID_{50} = 1$ is done. The values of I and [S] are calculated while the parameter X is varied in increments of 0.05. The results are listed in Table 1.

The values of I are plotted on the vertical axis of a semi-logarithmic graph, while the values of [S] are plotted on the horizontal axis. As a result, it is possible using an electronic calculator to obtain a theoretical S-curve of a competitive reaction reproducing the signal intensity I of the spin adducts $(T_{n_1}R_{m_1})$ observed according to variation of the scavenger concentration [S] as shown in Figure 1 as if obtained by computer simulation.

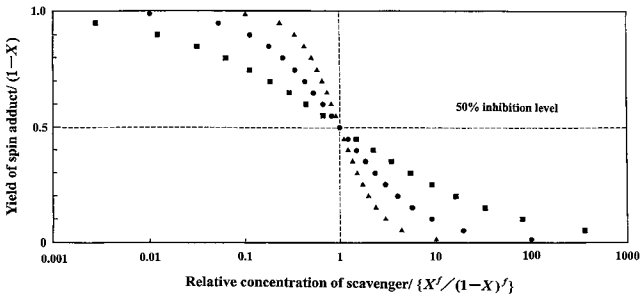

Figure 1. Variation of the S-shapes of the inhibition curves: $f = 0.5$ (▲), $f = 1$ (●), and $f = 2$ (■).

With respect to actually measured S-curves, it is known that S-curves of various slopes from various radical species were observed by Makino et al. in 1983,[5] by Mitsuta et al. in 1990[15] and 1994,[22] by Nishibayashi et al. in 1996,[28] by Sekine et al. in 1998,[23] by Asanuma et al. in 2001,[29] by Hamasaki et al. in 2008,[24] and by Komatsu-Watanabe et al. in 2008.[27]

In conclusion, the results are similar to the contents of the author's previous papers,[22,33] except that either eq 17 or 18 holds:

$$I = \frac{1}{m_1} \cdot I_{DMPO} \tag{17}$$

or

$$I = \frac{1}{m_1} \cdot (1-X) \cdot I_{DMPO,0} \tag{18}$$

where I_{DMPO} and $I_{DMPO,0}$ are spin adduct concentrations observed in the presence and absence of the scavenger S, respectively, using a spin-trapping agent like DMPO that induces a typical 1:1 reaction. I is the spin adduct concentration observed using spin-trapping agent T with $m_1 \neq 1$ when the scavenger S is present.

That is, the concentration I is $1/m_1$ of the spin adduct concentration I_{DMPO} of the spin-trapping agent DMPO that produces a typical 1:1 reaction. It is forecast that with respect to a spin-trapping agent (inducing reactions where $m_1 > 1$) that aggregates in, for example, an aqueous solvent, the spin adduct concentration after trapping will decrease according to the value of the parameter m_1. This is discussed in further detail in the next section.

Eliminating the parameter X from eqs 15 and 16 leads to the following relational equation:

$$[S] = \{(I_0/I) - 1\}^f \cdot ID_{50} \tag{19}$$

Taking logarithms of both sides yields

$$\log[S] = f \cdot \log\{(I_0/I) - 1\} + \log ID_{50} \tag{20}$$

Accordingly, if experimental values of log[S] are plotted on the vertical axis and experimental values of $\log\{(I_0/I) - 1\}$, on the horizontal axis, data points are arrayed in a straight line having an intercept of log ID_{50} and a slope of f. The value, f, of the scavenger can be experimentally determined from the slope f of the straight line.

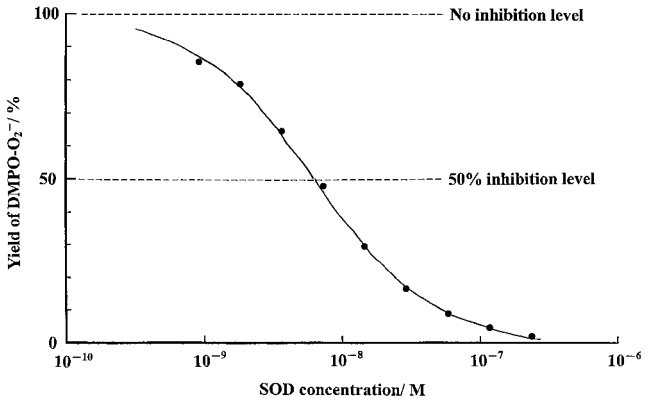

Figure 2. Inhibitory effect of SOD on the formation of DMPO–O_2^- observed in a hypoxanthine–XOD system at pH 7.8. The solid line shows the best-fitting curve obtained from the author's competitive reaction theory when three values of $m = 1$, $n = 1$, and $ID_{50} = 7.5 \times 10^{-9}$ M were assumed.

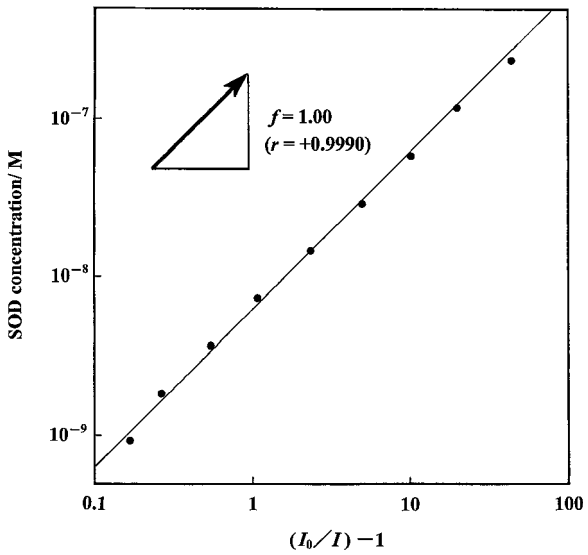

Figure 3. Relation between $\log\{(I_0/I) - 1\}$ and log[SOD] observed in a hypoxanthine–XOD system at pH 7.8. The correlation coefficient r is +0.9990.

The relational eqs 19 and 20 have exactly the same form as the previously derived relational eqs 14 and 15 of the author's second paper.[22] That is, in experiments where the concentration of the spin-trapping agent is kept fixed, the parameters m_1 and n_1 indicating aggregation of the spin-trapping agent are not reflected at all on the plotted graph when the f value of the scavenger is found.

In the purpose of explaining the slope variation of S-curves, the significance of this reaction model is to be able to characterize the complex competitive reaction systems macroscopically by using only a few parameters such as m_1, n_1, m_2, and n_2 when microscopic elementary processes of the reaction are unknown.

This general theory may seem complex at a first glance but if the four parameters m_1, n_1, m_2, and n_2 indicating aggregation are replaced by 1, it is obvious that this form assumes the same form of the simplest competitive reaction theory reported in 1990 by the present author and co-workers.[15] Two examples in which this theory is applied to actually obtained data are given below.

Bovine erythrocyte SOD (Cu,Zn-SOD) is a reference substance for scavengers in investigating the reactivity of biological substances with $O_2^{-\bullet}$. Accordingly, data about Cu,Zn-SOD is discussed first. Figure 2 is a graph showing an S-shaped curve that was reported in 1990 by the present author and co-workers.[15] The curve was obtained by competitively reacting Cu,Zn-SOD and DMPO with $O_2^{-\bullet}$ in a hypoxanthine–XOD system. Figure 3 is a graph obtained by converting these experimental values into a straight line having a slope of f and plotting the results on a double logarithmic graph. It can be seen from Figure 2 that the ID_{50} of Cu,Zn-SOD is 7.5×10^{-9} M. The experimental conditions show that [DMPO] is 0.67 M and k_{DMPO} is 18 $M^{-1} s^{-1}$ (at pH 7.8). Therefore, the second-order rate constant k_{SOD} for the reaction between Cu,Zn-SOD and $O_2^{-\bullet}$ is estimated to be 1.6×10^9 $M^{-1} s^{-1}$, using eq 13. It is observed from Figure 3 that the value of f results in $f_{SOD} = 1.00$ at a level of certainty indicated by the correlation coefficient $r = +0.9990$. Figure 3 shows that SOD did not show aggregation behavior when reacted with $O_2^{-\bullet}$.

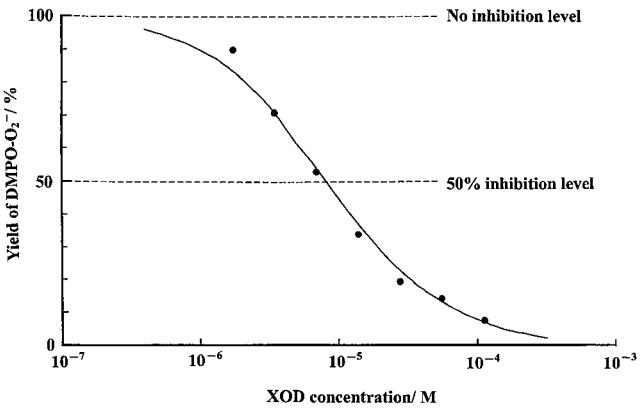

Figure 4. Inhibitory effect of XOD on the formation of DMPO–O_2^- observed in a KO_2 system at pH 7.8. The solid line shows the best-fitting curve obtained from the author's competitive reaction theory when three values of $m = 1$, $n = 1$, and $ID_{50} = 7.5 \times 10^{-6}$ M were assumed.

Figure 4 shows an S-shaped curve of the SOD-*like* activity of milk xanthine oxidase (XOD). The activity was measured using a KO_2 system established by the present author and co-workers in 1994.[22] The SOD-*like* activity possessed by the XOD itself cannot be measured except within a KO_2 system, because in a normally used hypoxanthine–XOD system, the measured XOD induces a reaction with the hypoxanthine of the system to thereby create $O_2^{-\bullet}$, hindering observation of the SOD-*like* activity.

It has been estimated from the results of experiments that the ID_{50} of XOD is 7.5×10^{-6} M (Figure 4). The experimental conditions show that [DMPO] is 0.60 M and k_{DMPO} is 18 $M^{-1} s^{-1}$ (at pH 7.8). Therefore, if an approximate relationship $m_2 = n_2 = 1$ is assumed, the second-order rate constant k_{XOD} for the reaction between XOD and $O_2^{-\bullet}$ is estimated to be 1.4×10^6 $M^{-1} s^{-1}$, using eq 13. If the local pH of the reaction field has been enhanced to about 10 because of the alkalinity of

the KO_2 itself,[21] the reaction rate constant k_{DMPO} on which the second-order rate constant for the reaction is based is ca. $10\,M^{-1}\,s^{-1}$ (at pH $\approx$10). k_{XOD} is reestimated to be ca. $8.0 \times 10^5\,M^{-1}\,s^{-1}$.

This value is equivalent to 0.88 to 0.50% of the k_{SOD} value of the reference material Cu,Zn-SOD measured in the hypoxanthine–XOD system. Thus, it can be said that XOD has a level of SOD-*like* activity that is several per thousand of the level of SOD activity of Cu,Zn-SOD. It is known that biological substances showing levels of SOD-*like* activity close to that of the XOD include cucumber ascorbate oxidase (AOD) and horse heart ferricytochrome *c* (Cyt. *c*). The SOD-*like* activity k_S of AOD is $4.8 \times 10^6\,M^{-1}\,s^{-1}$, and that of Cyt. *c*, $4.5 \times 10^5\,M^{-1}\,s^{-1}$, both at pH 7.8.[15,16] In other words, it can be said that XOD has a value of SOD-*like* activity equivalent to 33% to 17% of the activity of AOD and 3.6 to 1.8 times the activity of Cyt. *c*.

These values should never be ignored. There were reports in 1974 by Olson et al. that the amount of generation of $O_2^{-\bullet}$ observed in a xanthine–XOD system was smaller by one order of magnitude than the amount anticipated from the XOD reaction mechanism.[37,38] In these reports, Olson et al. have described this problem on the basis of their ESR rapid-freezing experiments as follows:

(1) "One of the most intriguing results is the relatively small amount of $O_2^{-\bullet}$ that is generated during the reaction of reduced xanthine oxidase with oxygen. If electrons were removed one at a time from fully reduced enzyme, 5 moles of $O_2^{-\bullet}$ per FAD would be produced in the fast phase. However, the observed amount is only 0.1 mole of $O_2^{-\bullet}$ per FAD. Even when this amount is corrected for the rate of disproportionation at pH 8.5 ($2 \times 10^5\,M^{-1}\,s^{-1}$) and for the fact that total reduction by xanthine was not achieved, the amount expected if oxygen removes electrons one at a time is still an order of magnitude greater than the observed. Furthermore, this small amount of $O_2^{-\bullet}$ is not easily explained in terms of the oxidation of partially reduced enzyme molecules with free superoxide anions since no effect of superoxide dismutase was observed on either the time course of the absorbance changes at low enzyme concentration or on the EPR signals at very high enzyme concentrations."[37]

(2) "The amount observed is still less than that predicted; however, the disparity (about a factor of 2) is much smaller than that if each step in reduction involved the production of $O_2^{-\bullet}$. For the latter case, the observed amount of $O_2^{-\bullet}$ is some 20 times less than that predicted. The reason for the small amount of observed $O_2^{-\bullet}$ remains unclear. It may be that xanthine oxidase itself exhibits some dismutase activity, particularly at the high enzyme and substrate concentrations used in the rapid freeze experiments."[38]

Judging from the results of our current experiments, one conceivable cause of this is the effect of $O_2^{-\bullet}$ eliminating activity (SOD-*like* activity) possessed by the XOD itself, as Olson et al. have already suggested.

Figure 5 is a graph obtained by converting the S-shaped curve of the XOD into a straight line having a slope of *f* and plotting the results on a double logarithmic graph. It can be seen from Figure 5 that the value of *f* of the XOD results in $f_{XOD} = 1.00$ at a level of certainty indicated by the correlation coefficient $r = +0.9881$. This value means that XOD does not show aggregation behavior when the XOD reacts with $O_2^{-\bullet}$, in the same way as in the case of Cu,Zu-SOD.

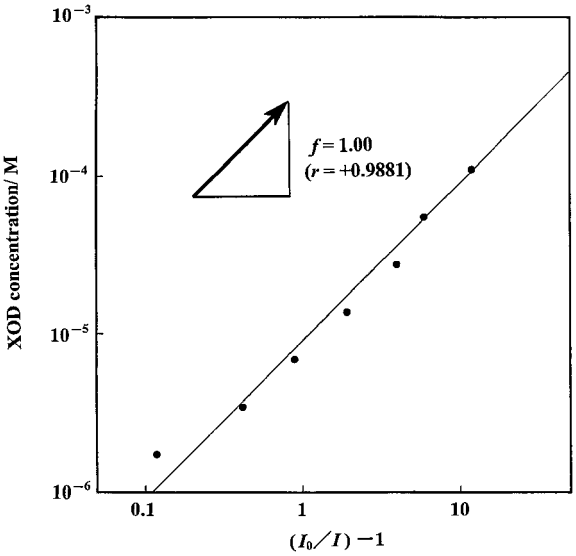

Figure 5. Relation between $\log\{(I_0/I) - 1\}$ and log[XOD] observed in a KO_2 system at pH 7.8. The correlation coefficient *r* is +0.9881.

New Theory Capable of Analyzing Saturation Level Curves Observed Prior to 1990 by the Present Author and Co-workers. In recent years, various spin-trapping agents have been synthesized and kinetically investigated by competitive reaction against a spontaneous dismutation of $O_2^{-\bullet}$ in water, and the rate constants for the reactions between the spin-trapping agents and $O_2^{-\bullet}$, k_T's, have been determined.[39–42] On the other hand, a traditional method for determining k_T's by using SOD or Cyt. *c* as a reference substance of a competitive reaction is also used by a few researchers.[43] Through these investigations, it has been clarified that the obtained k_T's had a great systematic error between the two methods. That is, strangely enough, the former k_T's are smaller by one order of magnitude than the latter.[39–44] In fact, such a strange phenomenon has been known partially since 1973.[11,45]

The author proposes a theory for analyzing a saturation level curve observed from a reaction competing between a radical elimination reaction where radicals spontaneously disappear from the system and a spin-trapping reaction where radicals are trapped by the spin-trapping agent without being eliminated from the system. The theory will be instrumental in characterizing the behavior of the spin-trapping agent and in understanding the cause of the above-mentioned great systematic error. Hitherto known examples of saturation level curves to be analyzed by the present theory include the saturation level curves observed by Sawada and Yamazaki in 1973[11] and by Nishikimi in 1975[12] in optical absorption spectroscopy and those obtained by Makino et al. in 1983,[5] by Mitsuta et al. in 1990,[15] and by Lauricella et al. in 2005[44] in spin-trapping methods.

The most general case [i.e., where radicals ($R^\bullet$) generated within a system react with, for example, the molecules of a solvent L (initial of the German word *Lösungsmittel*) constituting the whole system, spontaneously disappear, and some

of the radicals are trapped by the spin-trapping agent (T)] is first discussed. At this time, a reaction where radicals $R^\bullet$ are made to disappear by the solvent L and a reaction where radicals $R^\bullet$ are trapped by the spin-trapping agent T together constitute one competitive reaction. In this case, it is assumed that each reaction proceeds generally according to the ratio between m_1:n_1 and m_2:n_2, i.e., a complex non-stoichiometric reaction. Then,

$$m_1R^\bullet + n_1T \xrightarrow{k_T^*} (T_{n_1}R_{m_1}) \tag{21}$$

and

$$m_2R^\bullet + n_2L \xrightarrow{k_L^*} (L_{n_2}R_{m_2}) \tag{22}$$

Equation 21 indicates a non-stoichiometric spin-trapping reaction. Equation 22 indicates a non-stoichiometric reaction within the system in which radicals disappear spontaneously. The reaction rates of chemical reaction eqs 21 and 22 are naively and respectively assumed like the cases of eqs 4 and 5 as:

$$\frac{d[(T_{n_1}R_{m_1})]}{dt} = k_T^*[T]^{n_1}[R^\bullet]^{m_1} \tag{23}$$

and

$$\frac{d[(L_{n_2}R_{m_2})]}{dt} = k_L^*[L]^{n_2}[R^\bullet]^{m_2} \tag{24}$$

Where no spin-trapping agent is contained in the system, radicals are consumed by the reaction in eq 22. However, if a spin-trapping agent is added to the system, some of the radicals consumed by the reaction shown in eq 22 are consumed by a spin-trapping reaction of eq 21. Let Y ($0 < Y < 1$) be the ratio of radicals consumed by the spin-trapping reaction to the total amount of radicals consumed. When a spin-trapping agent is added, the ratio of radicals spontaneously disappearing and becoming consumed within the system can be represented as decreasing to $(1 - Y)$. Furthermore, the rate of consumption of the radicals depends on the ratios Y and $(1 - Y)$ at which the radicals are quenched by the molecules of the spin-trapping agent T and by those of the solvent L, respectively, and on the orders of reaction m_1 and m_2 of the radicals themselves. Therefore, the ratio of the rate of consumption induced by the radicals $R^\bullet$ and represented by the reaction rate eqs 23 and 24 can be represented by Y^{m_1}:$(1 - Y)^{m_2}$. It can be said from reaction eqs 21 and 22 that consumption of 1 mol of radicals $R^\bullet$ produces reaction products consisting of $1/m_1$ mole of $(T_{n_1}R_{m_1})$ and $1/m_2$ mole of $(L_{n_2}R_{m_2})$. Finally, the ratio of the reaction rate (23) and (24) to the rate of consumption of radicals are represented as follows according to a simple mass law:

$$-\frac{d[R^\bullet]}{dt} : \frac{d[(T_{n_1}R_{m_1})]}{dt} : \frac{d[(L_{n_2}R_{m_2})]}{dt} = 1 : \frac{1}{m_1}Y^{m_1} : \frac{1}{m_2}(1 - Y)^{m_2} \tag{25}$$

Equations 23, 24, and 25 lead to

$$k_T^*[T]^{n_1}[R^\bullet]^{m_1} : k_L^*[L]^{n_2}[R^\bullet]^{m_2} = \frac{1}{m_1}Y^{m_1} : \frac{1}{m_2}(1 - Y)^{m_2} \tag{26}$$

In order to facilitate the evolution of equations used later, a constant B is introduced such that $k_T^*[T]^{n_1}[R^\bullet]^{m_1} = (B/m_1)Y^{m_1}$ holds. Then, eq 26 may be rewritten as:

$$k_T^*[T]^{n_1}[R^\bullet]^{m_1} : k_L^*[L]^{n_2}[R^\bullet]^{m_2} = \frac{B}{m_1}Y^{m_1} : \frac{B}{m_2}(1 - Y)^{m_2} \tag{27}$$

When the relationship a:$b = c$:d holds, if $a = c$, then $b = d$. Therefore, if the terms a and c on the left are raised to the m_2th power and b and d on the right are raised to the m_1th power, the equality a^{m_2}:$b^{m_1} = c^{m_2}$:d^{m_1} also holds. Accordingly, eq 27 results in

$$\{k_T^*[T]^{n_1}[R^\bullet]^{m_1}\}^{m_2} : \{k_L^*[L]^{n_2}[R^\bullet]^{m_2}\}^{m_1} = \left\{\frac{B}{m_1}Y^{m_1}\right\}^{m_2} : \left\{\frac{B}{m_2}(1 - Y)^{m_2}\right\}^{m_1} \tag{28}$$

Because the product of the internal terms is equal to the product of the external terms, eq 28 can be modified to

$$k_L^{*m_1}[L]^{n_2m_1}[R^\bullet]^{m_1m_2} \cdot \frac{B^{m_2}}{{m_1}^{m_2}}Y^{m_1m_2} = k_T^{*m_2}[T]^{n_1m_2}[R^\bullet]^{m_1m_2} \cdot \frac{B^{m_1}}{{m_2}^{m_1}}(1 - Y)^{m_1m_2} \tag{29}$$

Rearranging eq 29 gives rise to

$$k_L^{*m_1} = k_T^{*m_2} \cdot B^{m_1-m_2} \cdot \frac{{m_1}^{m_2}}{{m_2}^{m_1}} \cdot \frac{(1 - Y)^{m_1m_2}}{Y^{m_1m_2}} \cdot \frac{[T]^{n_1m_2}}{[L]^{n_2m_1}} \tag{30}$$

In our experiments on competitive reactions for measuring saturation levels, the concentration of the spin-trapping agent was varied, while the amount of the solvent used in the system was kept constant. Therefore, when $Y = 0.5$ (i.e., 50% of the radicals generated within the system are trapped by the spin-trapping agent without disappearing spontaneously, in other words, spontaneous disappearance of the radicals within the system is limited to 50% by the spin-trapping agent), eq 30 is simplified into the following form by introducing ID_{50} (inhibitory dose fifty) into the variable concentration of the spin-trapping agent:

$$k_L^{*m_1} = k_T^{*m_2} \cdot B^{m_1-m_2} \cdot \frac{{m_1}^{m_2}}{{m_2}^{m_1}} \cdot \frac{{ID_{50}}^{n_1m_2}}{[L]^{n_2m_1}} \tag{31}$$

Comparing and combining eqs 30 and 31 gives rise to eq 32 or eq 33:

$$[T]^{n_1} = \frac{Y^{m_1}}{(1 - Y)^{m_1}} \cdot {ID_{50}}^{n_1} \tag{32}$$

or

$$[T] = \frac{Y^f}{(1 - Y)^f} \cdot ID_{50} \tag{33}$$

where the new factor f ($f = m_1/n_1$) is defined as the apparent number of radicals that one molecule of spin-trapping agent can trap. That is, aggregation behavior appears only on the spin-trapping agent side in this situation. In the experiments, the amount of solvent was kept constant and so m_2 and n_2, which are parameters indicating the aggregation behavior of the solvent molecules, are not reflected in the form of the saturation level curve.

Spin adduct concentrations $[(T_{n_1}R_{m_1})]$ obtained when the generated radicals $R^\bullet$ are trapped in part and in whole by the spin-trapping agent T are replaced by the signal intensities of the observed spin adducts $(T_{n_1}R_{m_1})$ represented by I and I_0,

respectively. Because of eq 25, the relationship between I and I_0 is given by

$$I = Y^{m_1} \cdot I_0 = Y^{m_1} \cdot \frac{1}{m_1} \cdot \int_0^t k_{\mathrm{DMPO}}[\mathrm{DMPO}][\mathrm{R}^\bullet]\mathrm{d}t \quad (34)$$

That is, the signal intensity I is represented as a function of Y and I_0. The concentration level I_0 at saturation remains equal to $1/m_1$ of the integral calculus value of the generating rate of the DMPO spin adduct that is generated from a typical 1:1 reaction. This is exactly the same phenomenon as was mentioned above using eqs 17 and 18.[46]

The Y of eqs 33 and 34 is used as a parameter for connecting I and [T]. The parameter Y is varied in increments of 0.05, and the values of I and [T] are computed. The computed values of I and [T] are plotted on the vertical axis and horizontal axis, respectively, of a graph. As a result, it is possible using an electronic calculator to obtain saturation level curves reproducing the signal intensities I of the spin adducts ($T_{n_1}R_{m_1}$) observed according to the variation of the spin-trapping agent concentration [T] as if obtained by computer simulation.

Tables 2–4 and Figures 6–8 show the results of calculations performed for various values of ID_{50}, m_1, and n_1. It can be seen from Table 2 and Figure 6 that, as the value of the ID_{50} of the spin-trapping agent decreases, the saturation level curve rises more steeply and the spin adduct concentration reaches its saturation level more quickly. Furthermore, it can be seen from Table 3 and Figure 7 that, as the degree of aggregation m_1 of radicals increases, the spin adduct concentration at the saturation level drops further. In addition, as can be seen from Table 4 and Figure 8, as the degree of aggregation n_1 of the spin-trapping agent increases, the rising portion of the saturation level curve from zero level resembles the S-shape more closely and the spin adduct concentration reaches its saturation level at a lower concentration of spin-trapping agent.

If it is possible to find the ratio of the saturation level concentration of the spin-trapped adduct which is formed from an m_1:n_1 reaction between radicals and a spin-trapping agent to

Table 2. Theoretically Calculated Values Illustrating Saturation Level Curves (When $m_1 = n_1 = 1$)

I		[T]		
Rate of trapping Y	Rate of disappearance $(1-Y)$	$\frac{Y}{(1-Y)} \cdot ID_{50}$		
		$ID_{50} = 1$	$ID_{50} = 5$	$ID_{50} = 10$
0	1.00	0	0	0
0.05	0.95	0.0526	0.2632	0.5263
0.10	0.90	0.1111	0.5555	1.1111
0.15	0.85	0.1715	0.8824	1.7647
0.20	0.80	0.2500	1.2500	2.5000
0.25	0.75	0.3333	1.6667	3.3333
0.30	0.70	0.4286	2.1429	4.2857
0.35	0.65	0.5385	2.6923	5.3846
0.40	0.60	0.6667	3.3333	6.6667
0.45	0.55	0.8182	4.0909	8.1818
0.50	0.50	1.0000	5.0000	10.000
0.55	0.45	1.2222	6.1111	12.222
0.60	0.40	1.5000	7.5000	15.000
0.65	0.35	1.8571	9.2857	18.571
0.70	0.30	2.3333	11.667	23.333
0.75	0.25	3.0000	15.000	30.000
0.80	0.20	4.0000	20.000	40.000
0.85	0.15	5.6667	28.333	56.667
0.90	0.10	9.0000	45.000	90.000
0.95	0.05	19.000	95.000	190.00

Table 3. Theoretically Calculated Values Illustrating Saturation Level Curves (When $ID_{50} = n_1 = 1$)

Rate of trapping Y	Rate of disappearance $(1-Y)$	I			[T]		
		$\frac{1}{m_1} \cdot Y^{m_1}$			$\frac{Y^f}{(1-Y)^f}$		
		$m_1 = 1$	$m_1 = 2$	$m_1 = 3$	$m_1 = 1$	$m_1 = 2$	$m_1 = 3$
0	1.00	0	0	0	0	0	0
0.05	0.95	0.05	0.0013	0.0000	0.0526	0.0028	0.0001
0.10	0.90	0.10	0.0050	0.0003	0.1111	0.0123	0.0014
0.15	0.85	0.15	0.0113	0.0011	0.1765	0.0312	0.0055
0.20	0.80	0.20	0.0200	0.0027	0.2500	0.0625	0.0156
0.25	0.75	0.25	0.0313	0.0052	0.3333	0.1111	0.0370
0.30	0.70	0.30	0.0450	0.0090	0.4286	0.1837	0.0787
0.35	0.65	0.35	0.0613	0.0143	0.5385	0.2900	0.1561
0.40	0.60	0.40	0.0800	0.0213	0.6667	0.4444	0.2963
0.45	0.55	0.45	0.1013	0.0304	0.8182	0.6695	0.5477
0.50	0.50	0.50	0.1250	0.0417	1.0000	1.0000	1.0000
0.55	0.45	0.55	0.1513	0.0555	1.2222	1.4938	1.8258
0.60	0.40	0.60	0.1800	0.0720	1.5000	2.2500	3.3750
0.65	0.35	0.65	0.2113	0.0915	1.8571	3.4488	6.4052
0.70	0.30	0.70	0.2450	0.1143	2.3333	5.4443	12.704
0.75	0.25	0.75	0.2813	0.1406	3.0000	9.0000	27.000
0.80	0.20	0.80	0.3200	0.1707	4.0000	16.000	64.000
0.85	0.15	0.85	0.3613	0.2047	5.6667	32.110	181.96
0.90	0.10	0.90	0.4050	0.2430	9.0000	81.000	729.00
0.95	0.05	0.95	0.4513	0.2858	19.000	361.00	6859.0

Table 4. Theoretically Calculated Values Illustrating the Saturation Level Curves (When $ID_{50} = m_1 = 1$)

I		[T]		
Rate of trapping Y	Rate of disappearance $(1-Y)$	$\frac{Y^f}{(1-Y)^f}$		
		$n_1 = 1$	$n_1 = 2$	$n_1 = 3$
0	1.00	0	0	0
0.01	0.99	0.0101	0.1005	0.2162
0.05	0.95	0.0526	0.2294	0.3748
0.10	0.90	0.1111	0.3333	0.4807
0.15	0.85	0.1765	0.4201	0.5609
0.20	0.80	0.2500	0.5000	0.6300
0.25	0.75	0.3333	0.5774	0.6934
0.30	0.70	0.4286	0.6547	0.7539
0.35	0.65	0.5385	0.7338	0.8136
0.40	0.60	0.6667	0.8165	0.8736
0.45	0.55	0.8182	0.9045	0.9353
0.50	0.50	1.0000	1.0000	1.0000
0.55	0.45	1.2222	1.1055	1.0692
0.60	0.40	1.5000	1.2247	1.1447
0.65	0.35	1.8571	1.3628	1.2292
0.70	0.30	2.3333	1.5275	1.3264
0.75	0.25	3.0000	1.7321	1.4422
0.80	0.20	4.0000	2.0000	1.5874
0.85	0.15	5.6667	2.3805	1.7828
0.90	0.10	9.0000	3.0000	2.0801
0.95	0.05	19.000	9.9499	2.6684

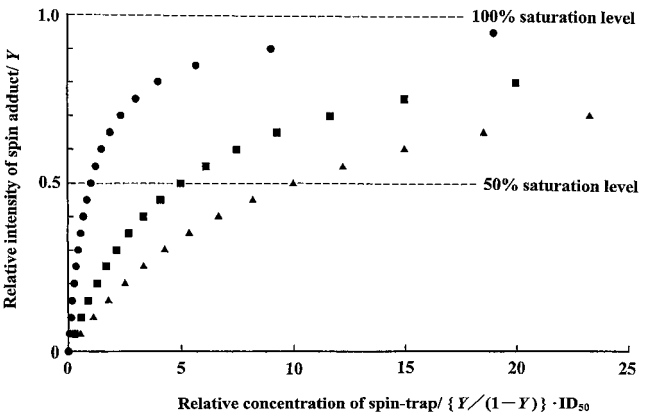

Figure 6. Theoretical intensity of the spin adducts as a function of the concentration of a spin-trapping agent when parameters m_1 and m_2 were set to 1: $ID_{50} = 1$ (●), $ID_{50} = 5$ (■), and $ID_{50} = 10$ (▲).

that of DMPO-type spin adduct which is formed from the 1:1 reaction between radicals and a spin-trapping agent, then the aggregation parameter of radicals m_1 can be found experimentally because the value of the denominator of the ratio is theoretically equal to m_1. This leads to the prediction that, with respect to a spin-trapping agent inducing a reaction with $m_1 > 1$, the spin adduct concentration observed after trapping radicals will decrease according to the degree of aggregation m_1 of radicals down to $1/m_1$. The presence of the factor m_1 might be one of the causes of the phenomenon of differing apparent spin adduct yields among different spin-trapping agents.

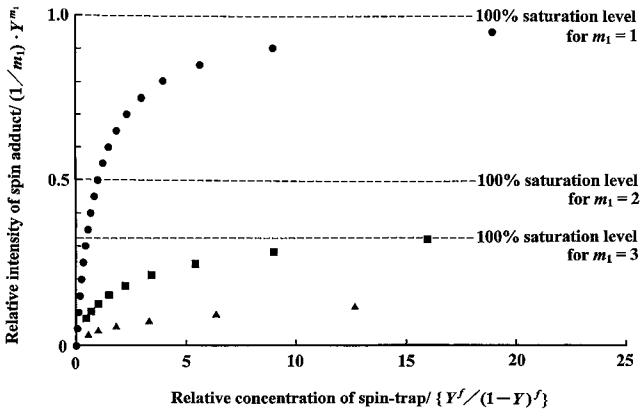

Figure 7. Theoretical intensity of the spin adducts as a function of the concentration of a spin-trapping agent when parameters ID_{50} and n_1 were set to 1: $m_1 = 1$ (●), $m_1 = 2$ (■), and $m_1 = 3$ (▲).

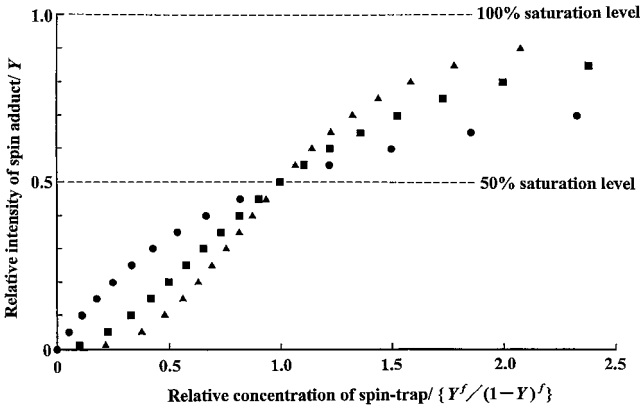

Figure 8. Theoretical intensity of the spin adducts as a function of the concentration of a spin-trapping agent when parameters ID_{50} and m_1 were set to 1: $n_1 = 1$ (●), $n_1 = 2$ (■), and $n_1 = 3$ (▲).

On the other hand, if a new spin-trapping agent inducing a reaction with $m_1 < 1$ is discovered, then development of an excellent spin-trapping agent will be achieved. That is, it is possible to perform a chemical amplification so that multiple molecules of spin adducts can be generated from one molecule of radical during radical trapping. If a spin-trapping agent producing a reaction with $m_1 < 1$ can be developed, there is a possibility that a high-sensitivity spin-trapping reaction could be accomplished. Please note that this is a theoretical prediction and may not be achievable in practice.

Eliminating the parameter Y from eqs 33 and 34 leads to the following relational equation:

$$[\mathrm{T}] = \left\{ \left(\frac{I_0}{I} \right)^{1/m_1} - 1 \right\}^{-f} \cdot \mathrm{ID}_{50} \tag{35}$$

Taking logarithms of both sides yields

$$\log[\mathrm{T}] = -f \cdot \log \left\{ \left(\frac{I_0}{I} \right)^{1/m_1} - 1 \right\} + \log \mathrm{ID}_{50} \tag{36}$$

Values of the m_1 are found from the experimental values of the saturation level and are substituted into eq 36. Experimental data can be organized on a double logarithmic graph in

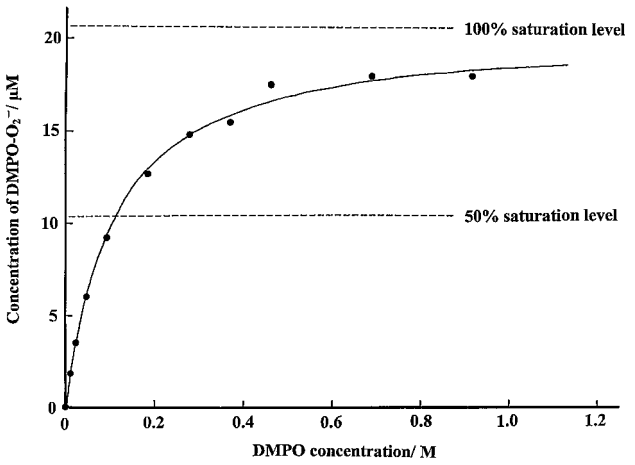

Figure 9. Experimental yields of DMPO–O_2^- as a function of the DMPO concentration observed in a hypoxanthine–XOD system at pH 7.8. The solid line shows the best-fitting curve obtained from the author's competitive reaction theory when four values of $m_1 = 1$, $n_1 = 1$, $ID_{50} = 1.1 \times 10^{-1}$ M, and $I_0 = 20.6$ μM were assumed.

which $\{(I_0/I)^{1/m_1} - 1\}$ is plotted on the horizontal axis and [T], on the vertical axis, on the basis of eq 36 having a set value of m_1. As a result, it can be predicted that experimental data points will be arrayed in a straight line having an intercept of log ID_{50} and a slope of $-f$. The value f of the spin-trapping agent can be determined experimentally from the obtained slope $-f$ of the straight line.

In the purpose of explaining the shape variation of saturation level curves, the significance of this reaction model is to be able to characterize the complex competitive reaction systems macroscopically by using only a few parameters such as m_1, n_1, m_2, and n_2 when microscopic elementary processes of the reaction are unknown.

In the case of a reaction between DMPO and $O_2^{-\bullet}$, it is considered that $m_1 = n_1 = 1$, i.e., $f = 1$. Therefore, eq 36 may be simplified as follows:

$$\log[T] = -\log\{(I_0/I) - 1\} + \log ID_{50} \quad (37)$$

Accordingly, it is possible to forecast that, if experimental values are plotted on a graph whose vertical axis represents log[T] and whose horizontal axis represents $\log\{(I_0/I) - 1\}$, then data points will be arrayed in a straight line having an intercept of log ID_{50} and a slope of -1.

Figure 9 shows an example of a saturation level curve obtained when $O_2^{-\bullet}$ spin adducts were produced in a hypoxanthine–XOD system, and reported in 1990 by the present author and co-workers.[15] The measurements were made using DMPO. Figure 10 is a both logarithmic graph obtained by plotting the experimental values based on the relation given by eq 37. As can be seen from Figure 9, the concentration level of DMPO–O_2^- approaches the 100% saturation level I_0 as closely as possible while a level of 20.6 μM is taken as an asymptotic line. As can be seen from Figure 10, when the saturation level of $O_2^{-\bullet}$ was actually set to a true saturation level I_0 of 20.6 μM based on a curve fitting method rather than an apparent saturation level of 18 μM, the experimental values were found to be precisely arrayed in a straight line having a

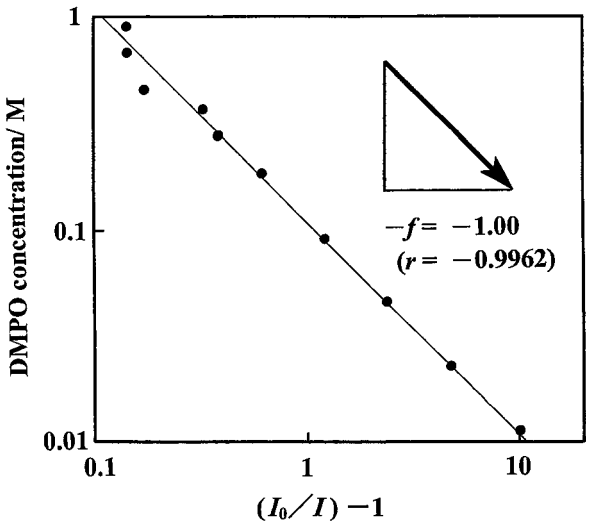

Figure 10. Relation between $\log\{(I_0/I) - 1\}$ and log[DMPO] observed in a hypoxanthine–XOD system at pH 7.8. The correlation coefficient r is -0.9962.

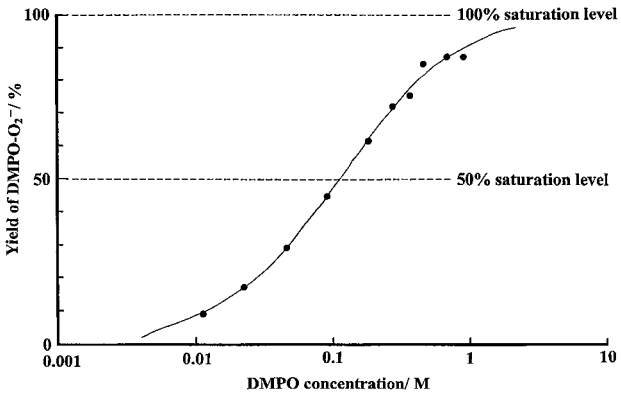

Figure 11. Experimental yields of DMPO–O_2^- as a function of log[DMPO] observed in a hypoxanthine–XOD system at pH 7.8. The solid line shows the best-fitting curve obtained from the author's competitive reaction theory when three values of $m_1 = 1$, $n_1 = 1$, and $ID_{50} = 1.1 \times 10^{-1}$ M were assumed.

slope of $-f = -1.00$ with a level of certainty given by the correlation coefficient $r = -0.9962$. In the case of DMPO, the slope of the graph demonstrates that the value of f is undoubtedly 1.

Mathematically, the saturation level curve is represented by a function having the same form as an S-curve drawn by a scavenger. Therefore, it can be postulated that the mode of plotting of the horizontal axis linear or logarithmic is the unique cause of the difference in appearance between the saturation level curve and the S-curve. To confirm this theory, the saturation level concentration was adjusted to 20.6 μM. In addition, the experimental values were re-plotted on a semi-logarithmic graph. The result is a typical S-curve representing the saturation level, as Figure 11 shows. The S-curve obtained from a competitive reaction between a scavenger and DMPO is a negative curve (i.e., it falls toward the right). On the other hand, the S-curve shown in Figure 11 is inverted relative to that, i.e., a positive curve (i.e., rising toward the right). It has

been confirmed that both types of S-curves are exactly identical in curvature.

If it is assumed that the reaction of the solvent L is a simple second-order reaction ($f = 1$) as well as a reaction of the spin-trapping agent DMPO, then a spin-trapping reaction and a reaction where radicals disappear spontaneously induces the following competitive reactions under conditions where the values of all four parameters m_1, n_1, m_2, and n_2 of eqs 21 and 22 are set to 1:

$$O_2^{-\bullet} + \text{DMPO} \xrightarrow{k_{\text{DMPO}}} \text{DMPO–}O_2^- \tag{38}$$

and

$$O_2^{-\bullet} + \text{L} \xrightarrow{k_{\text{L}}} \text{L-}O_2^- \tag{39}$$

where k_{L} is given by the following equation by setting the values of all of the four parameters m_1, n_1, m_2, and n_2 of eq 31 to 1:

$$k_{\text{L}} = k_{\text{DMPO}} \cdot \frac{\text{ID}_{50}}{[\text{L}]}. \tag{40}$$

From eq 40, k_{L} can be easily calculated roughly as the second-order rate constant for the reaction, based on [L], k_{DMPO}, and ID_{50} of DMPO. This approximated second-order rate constant, k_{L}, will become a good measure of reactivity when the reactivity between each radical species and each solvent molecule is examined. This is a significant point of this theory looked at from the viewpoint of practical use.

Now, it can be seen from Figures 9 and 11 that the concentration of DMPO at which spontaneous disappearance of $O_2^{-\bullet}$ within the system is reduced to 50%, i.e., the ID_{50} value, is 1.1×10^{-1} M. On the other hand, the conditions of the experiment show that the molar concentration of the aqueous solvent $[\text{L}] = [\text{H}_2\text{O}] = 55.6$ M. According to a published paper, $k_{\text{DMPO}} = 18\ \text{M}^{-1}\,\text{s}^{-1}$ (at pH 7.8).[15] Therefore, the rate constant k_{L} of a reaction in which radicals disappear spontaneously can be estimated from eq 40 to be $3.6 \times 10^{-2}\ \text{M}^{-1}\,\text{s}^{-1}$. This value is smaller than that in the literature for the rate constant $1.0 \times 10^5\ \text{M}^{-1}\,\text{s}^{-1}$ obtained for an $O_2^{-\bullet}$ disappearance reaction (at pH 7.8) by pulse radiolysis[47] by as much as 7 orders of magnitude. This extremely great difference may be the result of a phenomenon in which the chemical species L reacting with $O_2^{-\bullet}$ are, in fact, not water molecules but $O_2^{-\bullet}$ themselves, i.e., a dismutation reaction.

When k_{DMPO} is $18\ \text{M}^{-1}\,\text{s}^{-1}$ and the ID_{50} value of [DMPO] is 1.1×10^{-1} M, DMPO–O_2^- at a concentration level equivalent to a half of 20.6 μM is generated 85 s after the start of the reaction. Based on this fact, if the time course of the generation of DMPO–O_2^- is approximated by a straight line, $\text{d[DMPO–}O_2^-\text{]}/\text{d}t$ is calculated to be $1.2 \times 10^{-7}\ \text{M}\,\text{s}^{-1}$ by dividing 10.3 μM by 85 s. If based on this value, the steady-state concentration $[O_2^{-\bullet}]$ is estimated to be 6.1×10^{-8} M from the following equation:

$$\frac{\text{d[DMPO–}O_2^-\text{]}}{\text{d}t} = k_{\text{DMPO}}[\text{DMPO}][O_2^{-\bullet}] \tag{41}$$

Therefore, [L] of eq 40 can be replaced by $[O_2^{-\bullet}] = 6.1 \times 10^{-8}$ M. Then, recalculation using eq 40 indicates that the rate constant k_{L} for a reaction where radicals disappear spontaneously can be reestimated to be $3.2 \times 10^7\ \text{M}^{-1}\,\text{s}^{-1}$. This value is about 320 times the previously stated value from the literature, $1.0 \times 10^5\ \text{M}^{-1}\,\text{s}^{-1}$, which was obtained from a pulse radiolysis experiment.[47] It can be seen that the dismutation reaction rate of $O_2^{-\bullet}$ in our hypoxanthine–XOD system is much greater than those of $O_2^{-\bullet}$ dismutation reactions occurring in normal water.

This large value can be easily explained by assuming that the competition between a reaction where radicals disappear spontaneously and a spin-trapping reaction may in fact be a competition between an $O_2^{-\bullet}$ dismutation due to XOD and a spin-trapping reaction. If this value is calculated on the basis of the conclusion of the first section (i.e., the rate constant k_{XOD} for the reaction between XOD and $O_2^{-\bullet}$ is calculated to be $1.4 \times 10^6\ \text{M}^{-1}\,\text{s}^{-1}$) and also on the basis of eq 40 of the present section, the value may correspond to the dismutation reaction rate of $O_2^{-\bullet}$ when XOD at a concentration of $[\text{L}] = [\text{XOD}] = 1.4 \times 10^{-6}$ M is also present within the system. This value has validity because the final concentration of 0.083 unit/mL of XOD, being an experimental condition in our hypoxanthine–XOD system, is optically converted into a molar concentration of about 9.3×10^{-7} M that may be in agreement with the estimated XOD concentration of 1.4×10^{-6} M within the margin of experimental error.[48,49]

Consequently, $O_2^{-\bullet}$ can be considered to show high dismutation reaction rates in our hypoxanthine–XOD system, but this is greatly affected by the SOD-*like* activity which is possessed by the XOD itself and whose role is not yet known. The XOD reduces the amount of active oxygen species $O_2^{-\bullet}$, which are harmful and poisonous to a living body and are generated by the XOD itself. This means that the XOD's anti-oxidative activity is not visible and that that activity mainly contributes to eliminating $O_2^{-\bullet}$ from the hypoxanthine–XOD system. Furthermore, failure to observe this important SOD-*like* activity of XOD during these investigations and uncritically using a published value of k_{L} obtained from a pulse radiolysis experiment is likely to become one of the greatest causes of researchers' underestimation of k_{T}* by one order of magnitude when the method based on competitive reaction between a spin-trapping reaction for $O_2^{-\bullet}$ and the spontaneous dismutation of $O_2^{-\bullet}$ in the presence of XOD was used.[11,39–42,44]

Judging from the validity of the results of the above-described rough calculations, it has been found that the new theory established this time to analyze saturation levels may be one of the most important fundamental theories, as important as the already established theory for the evaluation of scavengers, for analyzing a competitive reaction system. Especially by using eq 40, it is possible to determine the unknown rate constants k_{L} for the spontaneous radical disappearance reaction in the various radical generating systems based on the known rate constant k_{T}. This value determined for the k_{L} will be a key to the investigation of the reaction mechanism of the main contributing spontaneous radical disappearance reaction in the system.

In conclusion, various competing reactions have been theoretically treated here. As a result, it has been found that the f value, which is a variable indispensable to the development of the theory described herein appears in various phases. Accordingly, the author proposes that the f value of a radical scavenging reaction caused by a scavenger observed in a

competitive reaction with a spin-trapping agent is termed f_S, while the f value of a spin-trapping reaction observed in an experiment for measuring the saturation level using a spin-trapping agent is termed f_T, in order to differentiate the two.

The completion of the theory of competitive reactions has greatly facilitated understanding of various phases not only of spin-trapping employing ESR spectroscopy and competitive reactions but also of various colorimetric methods employing optical absorption spectroscopy and competitive reactions. This theory can also be utilized analogically as a bio-mimetic reaction model for elucidating varied and complex competitive reactions occurring in a living body such as (1) an anti-oxidative response against oxidative stress, (2) an immune response occurring between an antigen and an antibody as a kind of competitive reaction, (3) an information transfer response occurring between a hormone, as one of the information transfer substances, and a hormone receptor as one of the hormone capture sites, (4) a pharmacological response involving the complex actions of agonists and antagonists on a drug receptor, and (5) an S-shaped dose-response curve after poison is taken and the lethal dose fifty (LD_{50}), as well as spin-trapping behavior observed in complex competitive reactions.

References

This paper is intended to be published in commemoration of the fiftieth birthday of the author and the twentieth anniversary of the author's first paper.

1 *Iwanami's Dictionary of Physics and Chemistry (Iwanami Rikagaku Jiten)*, 5th ed., Iwanami Shoten, Publishers, Tokyo, **1998**, pp. 331–332.

2 K. Mitsuta, in *Bioscience ESR 1*, ed. by H. Sakurai, Hirokawa Publishing Co., Tokyo, **1996**, pp. 74–88.

3 E. Finkelstein, G. M. Rosen, E. J. Rauckman, J. Paxton, *Mol. Pharmacol.* **1979**, *16*, 676.

4 a) E. Finkelstein, G. M. Rosen, E. J. Rauckman, *Arch. Biochem. Biophys.* **1980**, *200*, 1. b) E. Finkelstein, G. M. Rosen, E. J. Rauckman, *J. Am. Chem. Soc.* **1980**, *102*, 4994.

5 K. Makino, M. M. Mossoba, P. Riesz, *J. Phys. Chem.* **1983**, *87*, 1369.

6 This remarkable experimental fact was discovered first on January 30, 1986 by the author and was recorded in a paragraph of the day of the author's working diary.

7 a) M. Hiramatsu, R. Edamatsu, A. Mori, K. Mitsuta, M. Kohno, *Shinkei Kagaku* **1986**, *25*, 217. b) M. Hiramatsu, R. Edamatsu, M. Kohno, K. Mitsuta, A. Mori, *Neurochem. Res.* **1988**, *13*, 253, Abstract No. 65.

8 a) M. Hiramatsu, M. Kohno, *Nihon-Densi News* **1986**, *26*, 106. b) M. Hiramatsu, M. Kohno, *JEOL News* **1987**, *23A*, 7.

9 M. Hiramatsu, M. Kohno, R. Edamatsu, K. Mitsuta, A. Mori, *J. Neurochem.* **1992**, *58*, 1160.

10 H. Miyagawa, T. Yoshikawa, T. Tanigawa, N. Yoshida, S. Sugino, M. Kohno, *J. Clin. Biochem. Nutr.* **1988**, *5*, 1; The Stern–Volmer equation was originally developed for analyzing fluorescence quenching. See: O. Stern, M. Volmer, *Physik. Z. (Leipzig)* **1919**, *20*, 183.

11 Y. Sawada, I. Yamazaki, *Biochim. Biophys. Acta* **1973**, *327*, 257.

12 M. Nishikimi, *Biochem. Biophys. Res. Commun.* **1975**, *63*, 463.

13 M. Kohno, K. Mitsuta, Y. Mizuta, M. Hiramatsu, A. Mori, The 27th Annual Meeting of the Society of Electron Spin Resonance (The 27th ESR Touronkai), Sendai Municipal Museum Hall, Miyagi, Japan, October 27–29, **1988**, 29P02 (Abstracts pages 152–154).

14 K. Mitsuta, Y. Mizuta, M. Kohno, The 11th Annual Meeting of Japan Society of Magnetic Resonance for Life Science (The 11th Jikikyoumei Igakukai), Matsuyama Postal Savings Hall, Ehime, Japan, May 17–18, **1989**, 1P11 (Abstracts pages 92–95).

15 K. Mitsuta, Y. Mizuta, M. Kohno, M. Hiramatsu, A. Mori, *Bull. Chem. Soc. Jpn.* **1990**, *63*, 187.

16 K. Mitsuta, Y. Mizuta, M. Kohno, in *Magnetic Resonance and Medicine 1 (Jikikyoumei To Igaku 1)*, ed. by K. Ishizu, T. Yoshikawa, Nihon-Igakukan Co., Ltd., Tokyo, **1990**, pp. 113–117.

17 T. Hatano, R. Edamatsu, M. Hiramatsu, A. Mori, Y. Fujita, T. Yasuhara, T. Yoshida, T. Okuda, *Chem. Pharm. Bull.* **1989**, *37*, 2016.

18 M. Murakami, I. Zs.-Nagy, *Arch. Gerontol. Geriatr.* **1990**, *11*, 199.

19 K. Mitsuta, M. Kohno, Y. Mizuta, M. Yamada, M. Aoyama, in *Magnetic Resonance and Medicine 2 (Jikikyoumei To Igaku 2)*, ed. by E. Niki, K. Kakinuma, T. Yoshikawa, Nihon-Igakukan Co., Ltd., Tokyo, **1991**, pp. 190–195.

20 B. Gray, A. J. Carmichael, *Biochem. J.* **1992**, *281*, 795.

21 S. Kitagawa, H. Fujisawa, H. Sakurai, *Chem. Pharm. Bull.* **1992**, *40*, 304.

22 K. Mitsuta, M. Hiramatsu, H. Ohya-Nishiguchi, H. Kamada, K. Fujii, *Bull. Chem. Soc. Jpn.* **1994**, *67*, 529.

23 T. Sekine, T. Masumizu, Y. Maitani, T. Nagai, *Int. J. Pharm.* **1998**, *174*, 133.

24 T. Hamasaki, T. Kashiwagi, T. Imada, N. Nakamichi, S. Aramaki, K. Toh, S. Morisawa, H. Shimakoshi, Y. Hisaeda, S. Shirahata, *Langmuir* **2008**, *24*, 7354.

25 a) T. Tanigawa, *J. Kyoto Pref. Univ. Med.* **1990**, *99*, 133. b) L. Prónai, Y. Ichikawa, K. Ichimori, H. Nakazawa, S. Arimori, *J. Clin. Biochem. Nutr.* **1990**, *9*, 17.

26 R. Komatsu-Watanabe, Y. Sakurai, C. Morimoto, S. Sakamoto, K. Kanaori, K. Tajima, *Chem. Lett.* **2008**, *37*, 612.

27 N. Endo, S. Oowada, Y. Sueishi, M. Shimmei, K. Makino, H. Fujii, Y. Kotake, *J. Clin. Biochem. Nutr.* **2009**, *45*, 193.

28 S. Nishibayashi, M. Asanuma, M. Kohno, M. Gómez-Vargas, N. Ogawa, *J. Neurochem.* **1996**, *67*, 2208.

29 M. Asanuma, S. Nishibayashi-Asanuma, I. Miyazaki, M. Kohno, N. Ogawa, *J. Neurochem.* **2001**, *76*, 1895.

30 K. Satoh, Y. Ikeda, S. Shioda, T. Tobe, T. Yoshikawa, *Redox Rep.* **2002**, *7*, 219.

31 M. Kohno, M. Yamada, K. Mitsuta, Y. Mizuta, T. Yoshikawa, *Bull. Chem. Soc. Jpn.* **1991**, *64*, 1447.

32 S. Kohri, H. Fujii, S. Oowada, N. Endoh, Y. Sueishi, M. Kusakabe, M. Shimmei, Y. Kotake, *Anal. Biochem.* **2009**, *386*, 167.

33 K. Mitsuta, Y. Mizuta, M. Kusai-Yamada, M. Kohno, in *Magnetic Resonance and Medicine 3 (Jikikyoumei To Igaku 3)*, ed. by R. Ogura, T. Yoshikawa, Nihon-Igakukan Co., Ltd., Tokyo, **1992**, pp. 102–105.

34 F. A. Villamena, J. L. Zweier, *Antioxid. Redox Signaling* **2004**, *6*, 619.

35 *Nihon-Densi News* **1963**, *30*, 7.

36 J. M. McCord, I. Fridovich, *J. Biol. Chem.* **1969**, *244*, 6049.

37 J. S. Olson, D. P. Ballou, G. Palmer, V. Massey, *J. Biol. Chem.* **1974**, *249*, 4350.

38 J. S. Olson, D. P. Ballou, G. Palmer, V. Massey, *J. Biol. Chem.* **1974**, *249*, 4363.

39 A. Keszler, B. Kalyanaraman, N. Hogg, *Free Radical Biol. Med.* **2003**, *35*, 1149.

40 R. Lauricella, A. Allouch, V. Roubaud, J.-C. Bouteiller, B. Tuccio, *Org. Biomol. Chem.* **2004**, *2*, 1304.

41 A. Allouch, V. Roubaud, R. Lauricella, J.-C. Bouteiller, B. Tuccio, *Org. Biomol. Chem.* **2005**, *3*, 2458.

42 A. Allouch, R. P. Lauricella, B. N. Tuccio, *Mol. Phys.* **2007**, *105*, 2017.

43 J. Weaver, P. Tsai, S. Pou, G. M. Rosen, *J. Org. Chem.* **2004**, *69*, 8423.

44 R. P. Lauricella, J.-C. H. Bouteiller, B. N. Tuccio, *Phys. Chem. Chem. Phys.* **2005**, *7*, 399.

45 I. Yamazaki, L. H. Piette, T. A. Grover, *J. Biol. Chem.* **1990**, *265*, 652.

46 For example, unpublished data about 3,3,5,5-tetramethyl-1-pyrroline *N*-oxide (M_4PO). In the case of M_4PO, the value of m_1 seems to be larger than 1.

47 D. Behar, G. Czapski, J. Rabani, L. M. Dorfman, H. A. Schwarz, *J. Phys. Chem.* **1970**, *74*, 3209.

48 Milk xanthine oxidase is known to have an enzyme activity of more than 0.25 unit/mg protein and a molecular weight of ca. 300000. If 0.083 unit/mL XOD is converted into the molar concentration on the basis of these values, the result becomes ca. 1.1×10^{-6} M.

49 Based on eq 40 and the experimental conditions for 50% saturation (namely, $k_{DMPO} = 18\,M^{-1}\,s^{-1}$, $[DMPO] = 1.1 \times 10^{-1}$ M, and $[XOD] = 9.3 \times 10^{-7}$ M) in our hypoxanthine–XOD system, the second-order rate constant k_{XOD} for the reaction between XOD and $O_2^{-\bullet}$ is estimated to be roughly $2.1 \times 10^6\,M^{-1}\,s^{-1}$ at pH 7.8. This value is 1.5 to 2.6 times that of 1.4×10^6 or $8.0 \times 10^5\,M^{-1}\,s^{-1}$ estimated from our KO_2 system at pH 7.8. The cause of this difference seems to be the difference of the local pH of the reaction field in the early stage of the reaction between our two superoxide generating systems (Ref. 22).